INVESTIGATION OF ACOUSTIC EMISSION SIGNAL DURING LASER POWDER BED FUSION AT DIFFERENT OPERATING MODES

D. Kouprianoff[1]*

ARTICLE INFO

Article details
Presented at the 22nd Annual International Conference of the Rapid Product Development Association of South Africa (RAPDASA), held from 3-5 November 2021 in Pretoria, South Africa.

Available online 29 Nov 2021

Contact details
* Corresponding author
dkouprianoff@cut.ac.za

Author affiliations
1 Department of Mechanical and Mechatronic Engineering, Central University of Technology, South Africa

ORCID® identifiers
D. Kouprianoff
https://orcid.org/0000-0001-9409-8472

DOI
http://dx.doi.org/10.7166/32-3-2663

ABSTRACT

The increased use of metal additive manufacturing in production components makes quality control essential. The performance of parts produced by laser powder bed fusion depends on optimal process-parameters and the careful selection of scanning and building strategies for complex parts. In-situ acoustic emission provides a suitable solution for directly monitoring the laser powder bed fusion process during manufacturing. This paper shows the effect of different melting modes on the sound pressure and frequency spectrum during the laser powder bed fusion process. The results present valuable information for online monitoring development.

OPSOMMING

Die verhoogde gebruik van metaal toevoegingsvervaardiging in produksie onderdele maak gehaltebeheer noodsaaklik. Die werkverrigting van onderdele wat deur ‘n laserpoeierbed smeltproses vervaardig word, hang van optimale proses parameters en die noukeurige keuse van skandering- en boustrategieë vir komplekse onderdele af. In situ akoestiese emissie bied 'n geskikte oplossing vir die direkte monitor van die laserpoeierbed smeltproses. Hierdie artikel beskryf die effek van verskillende smeltmodusse op die klankdruk en frekwensie spektrum. Die resultate bied waardevolle inligting vir aanlyn moniteringsontwikkeling.

1 INTRODUCTION

Metal additive manufacturing (AM) has shown great application in industry. The metal AM market has grown more than 40% in the last 5 years [1]. The complex nature of the laser powder bed fusion (L-PBF) process makes slight variation in process variables detrimental to the quality of the parts. At a low laser energy density, a shallow wide track forms (conduction mode) and at a high energy density deep penetration occurs due to vapour recoil pressure which pushes back on the melt pool and forms a depression in the surface of the melt pool (keyhole mode). During keyhole mode, laser reflection within the cavity increases energy absorption. In the transition between the two modes the keyhole is present but has shallow penetration, characterised by a melt pool with an aspect ratio of ~1. The formation of defects during keyhole mode is dependent on various process parameters while the keyhole shape is greatly influenced by the speed of the laser. Formation of porosity in keyhole mode is attributed to an unstable melt pool that solidifies before the molten material can fill the cavity, trapping gas bubbles at the bottom [2]. Therefore, process monitoring for quality control of additive manufacturing is very important, especially for parts in safety critical applications. Gas-borne acoustic emission (AE) has been reported to be a feasible method for online monitoring of laser welding [3,4] and additive manufacturing processes, such as direct energy deposition [5] and laser powder bed fusion [6,7]. Acoustic emission generally refers to waves that arise from various energy sources which induce vibration or pressure waves which are monitored by a sensor and correlated to specific events. During additive manufacturing, some systems monitor the waves traveling through the substrate. Any energy released during the laser-material interactions, will be measured by the sensor. The use of acoustic and machine learning has been investigated for laser powder bed fusion; different porosity forming process parameters can be detected using machine learning [8-10]. Process monitoring for L-PBF is based on measuring various physical phenomena and correlating it to the process quality. Commercial L-

PBF process monitoring systems are still in its infancy and mostly makes use of cameras and pyrometry. Considerable work is needed to establish closed loop quality control [11]. This work sets out to show the correlation of audible acoustic emission of single tracks at different keyhole process parameters using an EOSINT M280 system.

2 METHODOLOGY

First, Ti6Al4V (ELI) powder and substrate was used for single track experiments. TLS Technik GmbH & Co. Spezialpulver KG (Germany) supplied a pre-alloyed gas atomised powder with the following chemical composition: Ti – balance, Al – 6,34%, V – 3,94%, O – 0,082%, N – 0.006%, H – 0,001%, Fe – 0,25%, C – 0.006% (weight %). The equivalent diameters (by volume) of the powder particles were d10 = 12 µm, d50 = 21 µm, and d90 = 31 µm.

The experiments were performed with an EOSINT M280; a microphone was placed inside the building chamber, 240 mm above the substrate. To achieve different modes of L-PBF, the laser power was varied between 100 W, 170 W, and 340 W, and the scanning speed was constant at 0.6 m/s. The optimal process parameters for this system were found to be at a laser power of 170 W with a scanning speed of 1.2 m/s [12] – that is, twice that used in this investigation. Two single tracks, 48 mm in length, were produced: one with powder and one without. The thicknesses of the powder layers were 1, 2, 4, 5, and 10 layers (a single layer's thickness being 30 µm). This resulted in two tracks positioned 40 mm apart for each layer, and a set of process parameters. First, two tracks were sintered without powder, then a powder layer was delivered, and the laser scanned two tracks next to the previous tracks (1mm apart). This procedure was repeated for the corresponding layers.

The AE was measured using an ICP microphone with an optimal frequency range of 3.75–20 000Hz (±2dB). The data was acquired at a sampling frequency of 102.5 kHz. For the analysis, post-processing was implemented using a 2 kHz high-pass filter to remove the effect of ambient operating noise that was unrelated to the laser scanning. Although some information might have been present below 2 kHz, it was not considered in this study. The data analysis was carried out using LabView and microscopy. Each track's corresponding sound waveform was extracted from the recording and analysed with Fast Fourier Transform (FFT), and the sound pressure level (SPL) was calculated. For optical microscopy, top and cross-sectional images were obtained. The data was used to correlate the track morphology with the frequency spectrum for the specific layer thickness.

3 RESULTS AND DISCUSSION

For the current system (EOSINT M280), the conduction mode was obtained at a laser power of 100 W, and the keyhole mode at a laser power of 170 W and 340 W (Figure 1). From the top view it can be seen that the track width for all of the laser powers was uniform throughout the length of the track. The depth of the tracks increased greatly with the increase in laser power.

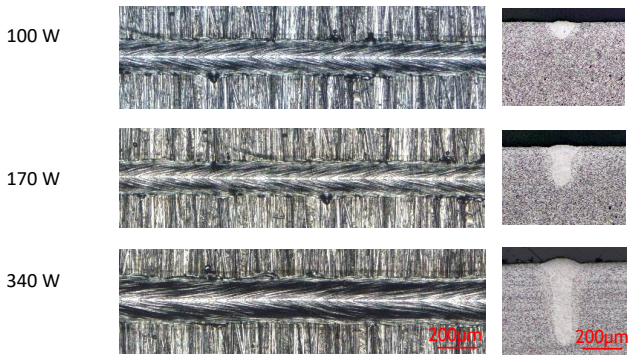

Figure 1: Top view and cross-sections of single tracks without powder at 100 W, 170 W, and 340 W laser power and 0.6 m/s scanning speed

Keyhole mode process parameters are undesirable, since they can cause porosity during the L-PBF process. At 340 W and 0.6 m/s, various defects were observed (Figure 2). Increase in layer thickness produced massive irregular tracks, with large volumes protruding above the substrate; and at 300 µm, unmelted particles were attached to the irregular track.

Figure 2: Cross-sections showing keyhole porosity and irregular surface of single tracks without powder (left), layer thickness of 120 µm (middle), and 300 µm (right) at 340 W laser power and 0.6 m/s scanning speed

At the laser power of 100 W and a powder layer thickness of 300 µm, the single tracks did not have contact with the substrate. A microscopic analysis of the tracks found that the contact zone decreased with increased layer thicknesses for all three laser powers. The contact zone was found to be the only dimension that had a distinct relationship with the sound pressure level. In Figure 3 it can be seen that the SPL decreases with a decrease in contact zone; note the increase for 100W at 30 µm. The width of the tracks followed the same pattern as the contact zone up to 120 µm; above 120 µm, 'ice cream cone'-shaped tracks formed, resulting in higher width measurements. At 30µm, 340W laser power produced a wider shallow track than those with the other layer thicknesses.

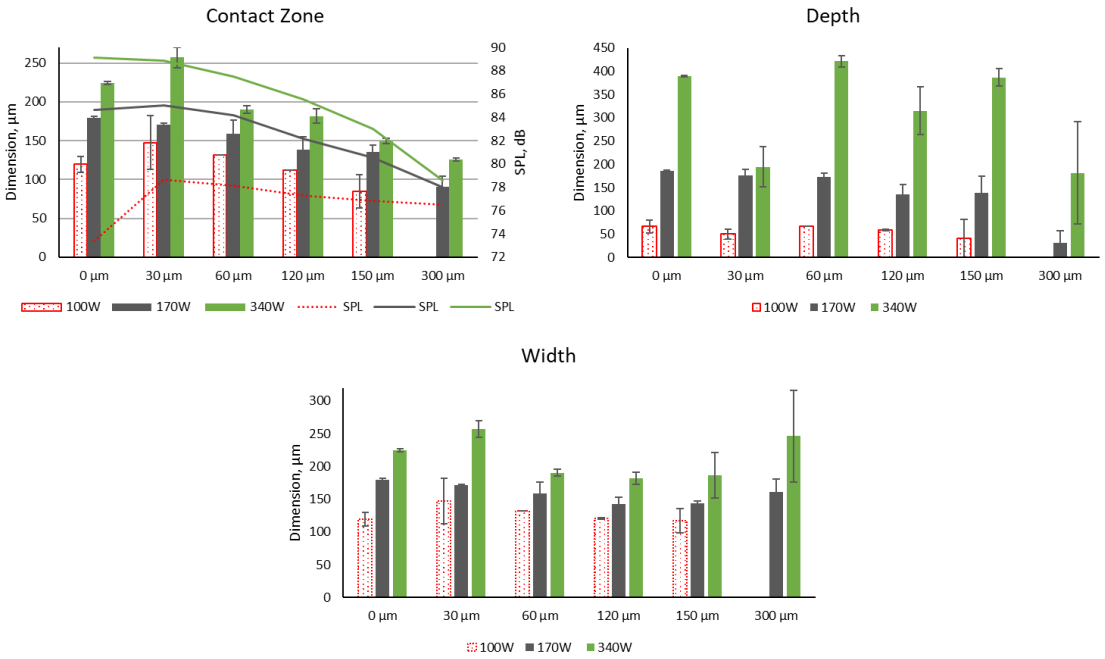

Figure 3: Geometrical characteristics of single tracks at different process parameters

The SPL was highest for 340W with no powder, at 89.58 dB. Figure 4 shows that the SPL increased with laser power and decreased with increasing powder thickness; the opposite results were found for 1.2 m/s [13], which showed that the SPL increased with powder layer thickness at a higher scanning speed of 1.2 m/s. This change in AE could be attributed to the melt pool dynamics, which change at higher scanning speeds [14].

The frequencies emitted at the two different keyhole parameters (170 W and 340 W at 0.6 m/s) were very similar (Figure 5). This suggests that, at these two parameters, the melt pool dynamics were similar and very stable. The same shape was present at both 170 W and 340 W (Figure 1), but 340 W showed a deeper penetration.

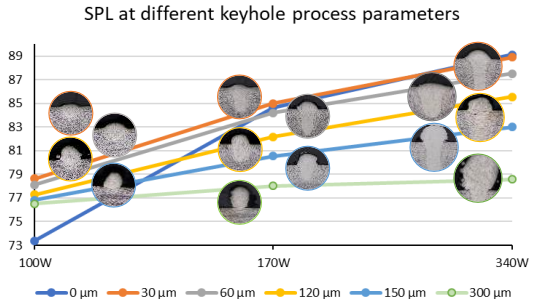

Figure 4: SPL of single tracks at 100 W, 170 W, and 340 W laser power and 0.6 m/s scanning speed. Cross-sections at corresponding layer thickness are shown

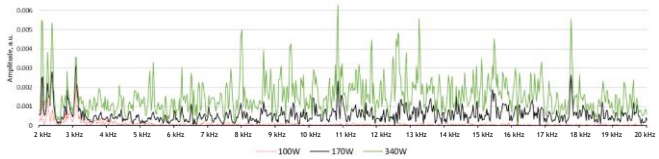

Figure 5: FFT spectrum of single tracks without powder at 100 W, 170 W, and 340 W laser power and 0.6 m/s scanning speed

For the 'no powder' case at 100 W, the linear energy density (P/V) was 166.667 J/m, resulting in conduction mode L-PBF. It is interesting that, for conduction mode produced with a similar linear energy density (P/V=141.7 J/m) but at a higher scanning speed (1.2m/s), a different frequency response was reported with a single high peak at ~7 kHz [13], which cannot be seen for 0.6 m/s (Figure 5). This implies that there is no definite clear relationship between AE spectral peak identification and the linear energy density. Each combination of process parameters produces a unique morphology of tracks and unique sound.

The FFT spectrum for the different laser powers had a similar shape, with the amplitude varying for 30 µm to 300 µm powder thickness. In Figure 6, at 300 µm the different laser power spectrums' shapes almost seem to merge. This is possibly because the melt pool loses contact with the substrate and cannot conduct heat away rapidly, leading to similar melt pool dynamics for the different laser powers.

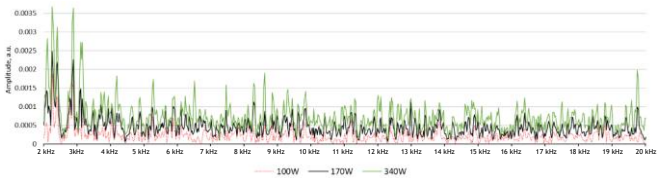

Figure 6: FFT spectrum single tracks with 300 µm powder layer thickness at 100 W, 170 W, and 340 W laser powers and 0.6 m/s scanning speed

4 CONCLUSION

Gas-borne acoustic emission results were reported for keyhole mode L-PBF. The sound pressure level decreased with increased layer thicknesses, and showed a relationship with the contact zone measurements. From this data it is clear that track morphology cannot be used alone to correlate to acoustic emission, but that one should also consider the different combinations of process parameters. The frequency response between 170 W and 340 W laser power is similar with varying amplitudes, which seem to merge as contact with the substrate is lost. Information about the acoustic emissions of different melting modes at different powder thicknesses could be valuable for increasing the probability of defect detection during online monitoring.

ACKNOWLEDGEMENT

This work was supported by the South African Research Chairs Initiative of the Department of Science and Technology and the National Research Foundation of South Africa (Grant No. 97994).

REFERENCES

[1] T. Wohlers. 2019. Wohlers Report 2019, “Additive manufacturing and 3D printing state of the industry,” Annual Worldwide Progress Report. Available: https://wohlersassociates.com/2019report.htm

[2] N. B. Dahotre and S. Harimkar, *Laser fabrication and machining of materials*, Springer Science & Business Media, 2008, https://doi.org/10.1007/978-0-387-72344-0

[3] L. Li and W. M. Steen, “Non-contact acoustic emission monitoring during laser processing,” International Congress on Applications of Lasers & Electro-Optics 1992, vol. 1(1), pp 719–728. https://doi.org/10.2351/1.5058543

[4] Y. Luo, L. Zhu, J. Han, X. Xie, R. Wan, and Y. Zhu, “Study on the acoustic emission effect of plasma plume in pulsed laser welding,” *Mechanical Systems and Signal Processing*, vol. 124, pp 715–723, 2019. https://doi.org/10.1016/j.ymssp.2019.01.045.

[5] H. Taheri, L. W. Koester, T. A. Bigelow, E. J. Faierson, and L. J. Bond, “In situ additive manufacturing process monitoring with an acoustic technique: Clustering performance evaluation using K-means algorithm,” *J. Manuf. Sci. Eng. Trans. ASME*, vol. 141(4), 2019. https://doi.org/10.1115/1.4042786

[6] M. R. Redding, S.A. Gold, and T. G. Spears, “Non-contact acoustic inspection method for additive manufacturing processes,” US Patent 20170146489, 2017.

[7] K. A. Fisher, J. V. Candy, G. Guss, and J. M. Mathews, “Evaluating acoustic emission signals as an in situ process monitoring technique for selective laser melting (SLM),” Technical Report No. LLNL-TR-706659, Lawrence Livermore National Lboratory, Livermore, 2016. https://doi.org/10.2172/1342013

[8] D. Ye, G. S. Hong, Y. Zhang, K. Zhu, and J. Y. H. Fuh, “Defect detection in selective laser melting technology by acoustic signals with deep belief networks,” *Int. J. Adv. Manuf. Technol.*, vol. 96, pp 2791–2801, 2018. https://doi.org/10.1007/s00170-018-1728-0

[9] S. A. Shevchik, C. Kenel, C. Leinenbach, and K. Wasmer, “Acoustic emission for in situ quality monitoring in additive manufacturing using spectral convolutional neural networks,” *Addit. Manuf.*, vol. 21, pp 598–604, 2018. https://doi.org/10.1016/j.addma.2017.11.012

[10] K. Wasmer, T. Le-Quang, B. Meylan, and S. A. Shevchik, “In situ quality monitoring in AM using acoustic emission: A reinforcement learning approach,” *J. Mater. Eng. Perform.*, vol. 28, pp 666–672, 2019. https://doi.org/10.1007/s11665-018-3690-2

[11] P. Yadav, O. Rigo, C. Arvieu, E. le Guen, and E. Lacoste, “In situ monitoring systems of the SLM process: On the need to develop machine learning models for data processing,” *Crystals*, vol. 10(6), 2020. https://doi.org/10.3390/cryst10060524

[12] I. Yadroitsava, J. Els, G. Booysen, and I. Yadroitsev, “Peculiarities of single track formation from TI6Al4V alloy at different laser power densities by selective laser melting,” *South African J. Ind. Eng.*, vol. 26(3), pp 86–95, 2015. https://doi.org/10.7166/26-3-1185

[13] D. Kouprianoff, I. Yadroitsava, A. du Plessis, N. Luwes, and I. Yadroitsev, “Monitoring of laser powder bed fusion by acoustic emission: Investigation of single tracks and layers,” *Frontiers in Mechanical Engineering*, vol. 7, 2021. https://doi.org/10.3389/fmech.2021.678076

[14] P. Bidare, I. Bitharas, R. M. Ward, M. M. Attallah, and A. J. Moore, “Fluid and particle dynamics in laser powder bed fusion,” *Acta Mater.*, vol. 142, pp 107–120, 2018. https://doi.org/10.1016/j.actamat.2017.09.051